Carbohydrate Research 373 (2013) 35–41

Contents lists available at SciVerse ScienceDirect

Carbohydrate Research

journal homepage: www.elsevier.com/locate/carres

Mutational analysis in the glycone binding pocket of *Dalbergia cochinchinensis* β-glucosidase to increase catalytic efficiency toward mannosides

Khakhanang Ratananikom [a], Khuanjarat Choengpanya [b], Nusra Tongtubtim [a], Theppanya Charoenrat [c], Stephen G. Withers [d], Prachumporn T. Kongsaeree [a,b,e,*]

[a] Department of Biochemistry, Faculty of Science, Kasetsart University, 50 Paholyothin Road, Ladyaw, Chatuchak, Bangkok 10900, Thailand
[b] Multidisciplinary Graduate Program in Genetic Engineering, Graduate School, Kasetsart University, Bangkok 10900, Thailand
[c] Department of Biotechnology, Faculty of Science and Technology, Thammasat University Rangsit Campus, Pathumthani 12120, Thailand
[d] Department of Chemistry, Faculty of Science, University of British Columbia, Vancouver, B.C., Canada V6T 1Z1
[e] Center for Advanced Studies in Tropical Natural Resources, NRU-KU, Kasetsart University, Bangkok 10900, Thailand

ARTICLE INFO

Article history:
Received 5 September 2012
Received in revised form 17 October 2012
Accepted 19 October 2012
Available online 27 October 2012

Keywords:
Abg
Catalytic efficiency
Dalcochinase
β-Glucosidase
Protein engineering

ABSTRACT

Dalcochinase and Abg are glycoside hydrolase family 1 β-glucosidases from *Dalbergia cochinchinensis* Pierre and *Agrobacterium* sp., respectively, with 35% sequence identity. However, Abg shows much higher catalytic efficiencies toward a broad range of glycone substrates than dalcochinase does, possibly due to the difference in amino acid residues around their glycone binding pockets. Site-directed mutagenesis was used to replace the amino acid residues of dalcochinase with the corresponding residues of Abg, generating three single mutants, F196H, S251V, and M369E, as well as the corresponding three double mutants and one triple mutant. Among these, the F196H mutant showed increases in catalytic efficiency toward almost all glycoside substrates tested, with the most improved catalytic efficiency being a 3-fold increase for hydrolysis of *p*-nitrophenyl β-D-mannoside, suggesting a preferred polar residue at this position and consistent with the presence of histidine at this position in two other GH1 glycosidases from barley and rice that prefer β-mannosides. In addition, the M369E mutation resulted in a small increase in catalytic efficiency for cleavage of *p*-nitrophenyl β-D-galactoside. By contrast, the multiple mutants were up to 8-fold less efficient than the recombinant wild-type dalcochinase, and displayed primarily antagonistic interactions between these residues. Thus, differences in catalytic efficiency between dalcochinase and Abg are therefore not primarily due to differences in the residues that directly contact the substrate, but derive largely from contributions from more remote residues and the overall architecture of the active site.

1. Introduction

β-Glucosidases (3.2.1.21) are a heterogeneous group of enzymes catalyzing the hydrolytic removal of β-D-glucose from the non-reducing end of β-D-glucosides and β-D-gluco-oligosaccharides. They are involved in various physiological processes, such as host defense mechanisms and growth control in plants, cellulose degradation in bacteria and fungi, and hydrolysis of glucosylsphingosine and glucosylceramide in humans. They have been classified into Carbohydrate Active EnZymes (CAZy) glycoside hydrolase (GH) families GH1, GH3, GH5, GH9, and GH30, based on amino acid sequence and structural similarity.[1–3] The GH1 family contains several activities, including β-glucosidases, β-mannosidases, β-fucosidases, β-galactosidases, and thioglucosidases. These enzymes have an $(\beta/\alpha)_8$ barrel structure with the conserved glutamate residues in the TL/FNEP and I/VTENG motifs, at the carboxyl-terminal ends of β-stands 4 and 7, acting as the catalytic acid/base and nucleophile, respectively, in the double displacement mechanism.[4,5] Apart from sharing overall structures, GH1 β-glucosidases from different sources also have similar functional properties, including optimal pH between 5 and 6 and molecular mass of about 55–65 kDa.[2]

Dalcochinase is a GH1 β-glucosidase from *Dalbergia cochinchinensis* Pierre (Thai rosewood).[6] Its natural substrate has been identi-

Abbreviations: GH, glycoside hydrolase; LFER, linear free energy relationships; *p*NP-α-L-Ara, *p*-nitrophenyl α-L-arabinoside; *p*NP-β-D-Fuc, *p*-nitrophenyl β-D-fucoside; *p*NP-β-D-Gal, *p*-nitrophenyl β-D-galactoside; *p*NP-β-D-Glc, *p*-nitrophenyl β-D-glucoside; *p*NP-β-D-Man, *p*-nitrophenyl β-D-mannoside; *p*NP-β-D-Xyl, *p*-nitrophenyl β-D-xyloside.

* Corresponding author. Tel.: +66 2 562 5555x2026; fax: +66 2 561 4627.
E-mail address: fscippt@ku.ac.th (P.T. Kongsaeree).

0008-6215/$ - see front matter © 2012 Elsevier Ltd. All rights reserved.
http://dx.doi.org/10.1016/j.carres.2012.10.018

fied as an isoflavonoid 12-dihydroamorphigenin-8′-O β-D-glucoside, also known as dalcochinin-8′-O-β-D-glucoside.[7] The pH optimum and an apparent molecular mass were reported as 5.5 and ≈330 kDa, respectively, and it was predicted to comprise 4–6 subunits of 66 kDa.[8] Amino acid sequence alignment has placed the catalytic acid/base and nucleophile residues at E182 and E396, respectively, comparable to other members of GH1.[6] Even though dalcochinase is defined as a β-D-glucosidase, it actually hydrolyzes *p*-nitrophenyl β-D-fucoside (*p*NP-β-D-Fuc) with 5-fold greater efficiency than *p*-nitrophenyl β-D-glucoside (*p*NP-β-D-Glc). Indeed, its specificity for the substituents at C-4 and C-6 positions is relatively lax since it hydrolyzes *p*-nitrophenyl β-D-galactoside (*p*NP-β-D-Gal), *p*-nitrophenyl α-L-arabinoside (*p*NP-α-L-Ara), and *p*-nitrophenyl β-D-xyloside (*p*NP-β-D-Xyl), albeit with 8- to 80-fold lower efficiency than the glucoside.[8]

Abg is another GH1 β-glucosidase from *Agrobacterium* sp. It comprises a homodimer with 51 kDa subunits.[9,10] The acid/base and nucleophile residues were identified as E170 and E358, respectively, by site-directed mutagenesis and labeling with the mechanism-based inactivator.[11,12] Abg also cleaves a range of *p*-nitrophenyl glycosides, with *p*NP-β-D-Glc being the best substrate and others cleaved about 2- to 360-fold slower. Abg also hydrolyzes *p*-nitrophenyl β-D-mannoside (*p*NP-β-D-Man) very slowly, with a k_{cat}/K_m value of 6 mM^{-1} s^{-1}, which is unusual among β-glucosidases since hydrogen bond interactions between the C2-hydroxyl group and the residues in the active site pocket of the enzyme contribute directly to transition state stabilization.[13–15]

While sharing 35% sequence identity, Abg was 4- to 40-fold more efficient than dalcochinase for the same *p*-nitrophenyl glycoside substrates. For *p*NP-β-D-Glc, where the difference in efficiency was greatest, the k_{cat} of Abg was only 2-fold lower, but its K_m was 70-fold lower than that of dalcochinase. For *p*NP-β-D-Fuc, where the difference in efficiency was the smallest, their k_{cat} values are very close, but the K_m of Abg was 5-fold lower than that of dalcochinase. These parameters suggest that the differences in catalytic efficiencies between these two enzymes are dominated by the glycosylation step (reflected by the values of k_{cat}/K_m) over the deglycosylation step (reflected by the values of k_{cat}), possibly reflecting differences in the amino acid residues that form direct and/or indirect interactions with the glycone moieties in their respective active site pockets.

X-ray crystallography and site-directed mutagenesis studies of various β-glucosidases showed that the residues involved in aglycone binding are variable in GH1 β-glucosidases, whereas those interacting with the glycone moiety are mostly conserved.[16–24] However, there are examples of unique residues in the glycone binding pocket that are important for determining glycone specificity. Exchanges of active site residues N206D in *Pyrococcus furiosus* β-glucosidase and D206N in *Pyrococcus horikoshii* β-mannosidase increased their preference for mannoside and glucoside substrates, respectively.[25] Also, the W433C substitution in *Sulfolobus solfataricus* β-glycosidase resulted in 24-fold increase in its preference for mannoside over galactoside substrates.[18,44]

Here, the amino acid residues that might be responsible for the difference in catalytic efficiencies between dalcochinase and Abg were probed by site-directed mutagenesis to generate single, double, and triple dalcochinase mutants. Their kinetic analysis enabled an evaluation of the interaction strengths between a pair of mutations in multiple mutants, and the active site similarity between the wild-type and mutant enzymes via linear free energy relationships (LFER). Our results highlighted the preference for histidine at position 196 instead of phenylalanine for hydrolysis of a β-mannoside substrate. However, most mutations displayed antagonistic interactions, and none could generate an active site that resembled the active site architecture of Abg. So, substrate specificity is likely determined by specific residues as well as the overall interactions in the active site pockets (including both glycone and aglycone subsites). Together these results allow us to better understand the roles of specific amino acid residues around the glycone pocket of dalcochinase and Abg, and provide information for future protein engineering of GH1 β-glucosidases with an improved catalytic efficiency.

2. Experimental procedures

2.1. Strains, plasmids, and chemicals

Escherichia coli strain DH5α and *Pichia pastoris* strain Y11430 (Invitrogen, Carlsbad, CA, USA) were used for plasmid propagation and protein expression, respectively. The recombinant plasmid pPICZ-His_8-trncTRBG that harbors the coding sequence of N-terminally truncated form of dalcochinase (starting from the residue V14 of the mature sequence) following the α mating factor propeptide and 8 histidine residues, was used for the expression of the recombinant wild-type dalcochinase.[26] *Pfu* DNA polymerase and *Dpn*I were purchased from Promega (Madison, WI, USA). All *p*-nitrophenyl glycoside substrates were purchased from Sigma (St. Louis, MO, USA).

2.2. Sequence alignment, homology modeling, and molecular docking

The sequences of dalcochinase, Abg, and other GH1 β-glycosidases were aligned using ClustalW 2.0.12.[27] The homology model of dalcochinase was generated by MODELLER 9v4 program,[28] using the structure of cyanogenic β-glucosidase from *Trifolium repens* L. (white clover) (PDB code 1CBG) as a template.[16] The overall structure of the model was checked by the PROCHECK, ProSA, Verify-3D, and WHATIF programs.[29–31] The active site was defined as 15 Å around the pseudo-atom which was generated at the center of catalytic residues, E182 and E396, of dalcochinase.

The structure of gluconolactone (PDB code LGC) was docked into the active site of modeled dalcochinase using AutoDock version 4.2. The coordinate files of both protein and ligand required for docking calculation were prepared by AutoDockTools. The non-polar hydrogens were deleted by the program, and the partial charges were merged to the carbon atoms. The sugar substrates were treated as rigid, and the rotatable bonds were set automatically by the program. The protein portion was set as flexible receptor by assigning the predicted catalytic residues (E182 and E396) as flexible residues. AutoGrid was performed to pre-calculate the grid map of interaction energy prior to docking. The grid size was set at 60 × 60 × 60 with a grid point spacing of 0.258 Å at the center of protein. A Lamarckian genetic algorithm was used with a population size of 300, maximum number of energy evaluations of 2,500,000, maximum number of generations of 25,000, and uniform crossover mode. Other parameters were set as default. The docked conformation was visualized using Accelrys DS Visualizer 3.0 (Accelrys Inc., San Diego, USA).

2.3. Construction of dalcochinase mutants

The dalcochinase mutants were made via site-directed mutagenesis to replace amino acid residues at the positions F196, S251, and M369 of dalcochinase (the numbers indicate their positions in the reported sequence of dalcochinase[6]) with the corresponding residues of Abg, to generate three single mutants F196H, S251V, and M369E, three double mutants F196H/S251V, F196H/M369E, and S251V/M369E, and one triple mutant F196H/S251V/M369E. The specific primers for each mutant were designed based on the dalcochinase cDNA sequence (Genbank accession

AF163097).[6] The sequences of the sense mutagenic primers of F196H, S251V, and M369E were 5′-GGGTATGCATACGGTATGCATGCACCAGGTCGATGTTCTCC-3′, 5′-CATCAGAAAGGTACAATAGGCATTGTTTTGCACGTAGTTTGGG-3′, and 5′-GGTCCAGTGACTCCCTCAGGATGGGAATGCATTTATCCAAAAGG-3′, respectively (mutation sites are underlined). Sequences of the antisense mutagenic primers are the reverse complements of the sequences shown above. The recombinant plasmid pPICZ-His$_8$-trncTRBG was used as a template for generating single mutations. The plasmids harboring single and double mutations were used as a template for generating double and triple mutations, respectively. Site-directed mutagenesis reactions were performed with 3 units *Pfu* DNA polymerase according to the method published previously.[32] The reactions were incubated with 10 units *Dpn*I at 37 °C overnight to remove the DNA template. The *Dpn*I-treated DNA was transformed into competent *E. coli* by electroporation. The transformants were selected on LB-agar plates containing 25 μg/mL zeocin at 37 °C. The plasmids containing correctly mutated dalcochinase sequences were checked by DNA sequencing. Subsequently, the mutant plasmids were linearized with *Sac*I, transformed into *P. pastoris* by electroporation, and selected on YPDS plates with 100 μg/mL zeocin, following the protocols from Invitrogen.

2.4. Expression and purification of enzymes in *P. pastoris*

The wild-type and mutant forms of dalcochinase were expressed in a 2-liter Biostat B fermenter (B. Braun Biotech International, Germany), or in a shake-flask system as described previously.[26,33] Then, enzymes were purified from the culture media by hydrophobic interaction chromatography followed by immobilized metal-ion affinity chromatography.[26]

Protein concentration determination was performed according to the Bradford method by using the BioRad Protein Assay Reagent Kit (Bio-Rad, Hercules, CA, USA) and bovine serum albumin as a standard. SDS–PAGE was performed in a discontinuous system with 4.5% separating and 7.5% resolving gel.[34] Western blot analysis and chemiluminescent detection were done with mouse monoclonal antibody against natural dalcochinase (a gift from Professor Watchara Kasinrerk, Chiangmai University, Thailand), horseradish peroxidase-conjugated rabbit polyclonal antibody against mouse immunoglobulin (Dako, Glostrup, Denmark), and ECL Plus Western Blotting Detection reagents (GE Healthcare, Buckinghamshire, UK). To remove conjugated oligosaccharides, the glycosylated proteins were treated with endoglycosidase H$_f$ (New England BioLabs, USA) for 2 h at 37 °C under denaturing conditions according to manufacturer's instructions.

2.5. Kinetic measurements

The catalytic efficiencies (k_{cat}/K_m) of the wild-type and mutant forms of dalcochinase for hydrolysis of various *p*NP-glycoside substrates were determined from progress curves at low substrate concentrations (less than 1/5 K_m of wild-type dalcochinase toward the same substrate) in 0.1 M sodium acetate, pH 5.0 at 30 °C. The *p*-nitrophenol released was monitored by following the absorbance at 360 nm until substrate depletion was observed. When the substrate concentration is low, the rate of reaction (v) is related to the substrate concentration by the equation:[35]

$$v = (k_{cat}/K_m)[E]_0[S] \quad (1)$$

The change in absorbance with respect to time was fitted to first-order rate equation using the program GraFit 5.0 (Erithacus Software Limited, Horley, UK) to yield pseudo-first-order rate constant that corresponds to (k_{cat}/K_m) $[E]_0$. Since $[E]_0$, which was the concentration of enzyme used in the reaction, was known, the value of k_{cat}/K_m could be easily obtained.

2.6. Calculation of activation free energy changes

The difference in the activation free energy ($\Delta\Delta G^{\ddagger}$) for the glycosylation step of hydrolysis was calculated by the following equation:[36]

$$\Delta\Delta G^{\ddagger} = -RT\ln[(k_{cat}/K_m)_1/(k_{cat}/K_m)_2] \quad (2)$$

where R is the gas constant (8.314 Jmol^{-1}), T is the absolute temperature (303 K), and k_{cat}/K_m is rate constant of the hydrolysis of the same substrate by two different enzymes.

3. Results and discussion

3.1. Homology modeling, molecular docking, and sequence alignment

Since the 3-dimensional structures of both dalcochinase and Abg are lacking, despite our efforts over several years, the homology model of dalcochinase was generated (Supplementary Fig. 1) using the structure of white clover β-glucosidase as a template since it shows the highest sequence similarity (59%).[16] The selected model showed the root mean square deviation of the Cα atoms of 0.39 Å with respect to the template, and satisfied all criteria as evaluated by PROCHECK, ProSA, Verify-3D, and WHATIF programs (Supplementary Table 1). The slot-like binding pocket of dalcochinase was approximately 22 Å long and 8 Å wide (calculated from distances between P347-Cγ and E455-Oε2, and between N189-Nδ2 and W368-Cδ1, respectively), with the catalytic amino acid residues located about 5.5 Å apart (between E182-Oε1 and E396-Oε1) at the bottom of the binding pocket. In order to predict the interactions between the enzyme and the glycone substrate, gluconolactone, which mimics the proposed $^4H_3$ half chair transition-state conformation of the glucose substrate,[44] was docked into the active site pocket of the dalcochinase model (Fig. 1). Gluconolactone appeared to form hydrogen bonds with residues Q36, N181, E182, E452, and W453 of dalcochinase, and the distances between the docked gluconolactone and the amino acid residues in the glycone binding pocket of dalcochinase model as predicted by molecular docking are summarized in Supplementary Table 2.

From the docked position of gluconolactone, 17 residues were predicted to be located in the glycone binding pocket of dalcochinase (Fig. 1). Among these, 14 residues are similar between dalcochinase and Abg, namely Q36, R90, H136, W137, N181, E182, N323, Y325, W368, E396, W445, E452, W453, and F461 in dalcochinase, corresponding to Q24, R81, H125, W126, N169, E170, N296, Y298, W331, E358, W404, E411, W412, and F420 in Abg, respectively (Supplementary Fig. 2). In many cases, their corresponding positions in other GH1 β-glucosidases have been reported to make direct contacts with the glucosyl moiety in the -1 subsite. The two catalytic acid/base and nucleophile residues are universally conserved in all GH1 enzymes as expected,[2] with the exception of myrosinases.[37] The residues Q39 and E451 in *Spodoptera frugiperda* β-glycosidase, corresponding to Q36 and E452 in dalcochinase, respectively, were found to interact with the hydroxyl groups at C3, C4, and C6, of the glycone moiety of the substrate.[19] The residues R77 and N206 in *Pyrococcus furiosus* β-glucosidase, corresponding to R90 and N181 in dalcochinase, respectively, were shown to interact with the catalytic nucleophile and the equatorial C2-hydroxyl group of the non-reducing end sugar.[25] The residues H142 and W457 in *Zea mays* (maize) β-glucosidase, corresponding to H136 and W445 in dalcochinase,

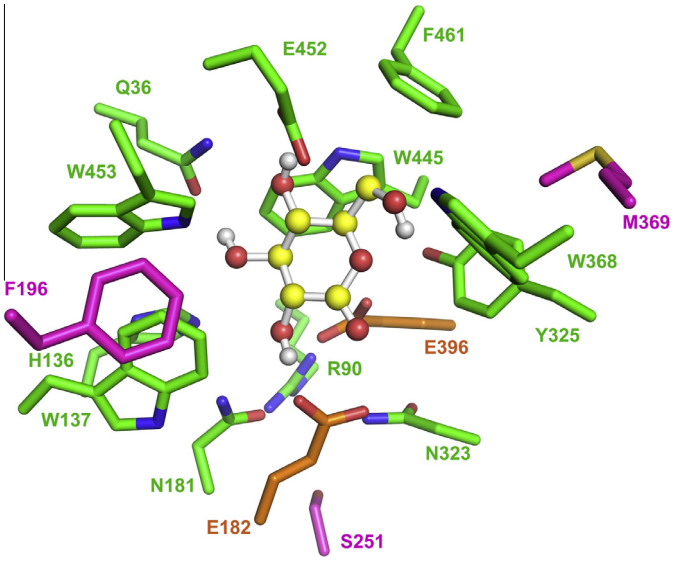

Figure 1. The homology model of wild-type dalcochinase containing a docked structure of gluconolactone. The model is shown as viewed from the exterior of the enzyme, looking into the active site pocket. The main chain conformation is omitted. The catalytic acid/base and nucleophile at E182 and E396, respectively, are shown as orange stick models. The 12 other residues that are likely located in the glycone binding pocket of dalcochinase and are similar between dalcochinase and Abg, are shown as green stick models, while the three residues in dalcochinase that are targeted for site-directed mutagenesis (F196, S251, and M369) are shown as pink stick models. The docked gluconolactone is shown as a yellow ball-and-stick model. The picture was generated with PyMOL version 1.3 (DeLano Scientific, Palo Alto, CA, USA). (For interpretation of the references to colour in this figure legend, the reader is referred to the web version of this article.)

respectively, were shown to make hydrogen bond interactions with the glycone moiety in its active site pocket.[17] The residue W433 in *Sulfolobus solfataricus* β-glycosidase, corresponding to W453 in dalcochinase, was shown to form hydrogen bonds to the C3-hydroxyl group of the sugar substrate.[18]

While the conservation of amino acid residues that make up the glycone binding pockets of various GH1 β-glucosidases is indicative of their specificity for the β-glucoside substrate, the slight variations in surrounding residues may subtly affect their interactions with the glycone moiety. In this study, 3 out of 17 residues that were likely located in the glycone binding pocket of dalcochinase, were different between dalcochinase and Abg, namely F196, S251, and M369 in dalcochinase, corresponding to H184, V224, and E332 in Abg, respectively (Fig. 1 and Supplementary Fig. 2). In the docking model, the residue F196 points toward the C2-hydroxyl group of the docked gluconolactone. The residue S251, while appearing to be far from the docked structure, corresponds to the residue V241 of *Oryza sativa* L. (rice) Os3BGlu7, that is in direct contact with the sugar moiety in the -1 subsite.[38] The residue M369 is close to the C6-hydroxyl group of the docked gluconolactone. Therefore, these amino acid residues in dalcochinase were replaced with the corresponding residues of Abg by site-directed mutagenesis to see if these made the enzyme more Abg-like and resulted in activity increases. In total, three single mutants F196H, S251V, and M369E, three double mutants F196H/S251V, F196H/M369E, and S251V/M369E, and one triple mutant F196H/S251V/M369E, were generated.

3.2. Production of dalcochinase mutants

All dalcochinase mutants were produced in *P. pastoris*, and purified using two chromatographic steps. Purification yields and specific activities of mutants range from 11% to 60% and 1–10 μmol min^{-1} mg^{-1}, respectively. All dalcochinase mutants exhibited a broad band of about 66 kDa on SDS–PAGE, which is similar to the recombinant wild-type dalcochinase (Supplementary Fig. 3) but different from a sharp protein band at 60 kDa of natural dalcochinase.[26,32] The broad protein bands could be sharpened by treatment with endoglycosidase H_f (Supplementary Fig. 4), and thus are likely due to greater glycosylation in yeast than in plants.[39] Detection of these bands with mouse monoclonal antibody against natural dalcochinase in a Western blot confirmed their identity as dalcochinase proteins (Supplementary Fig. 3).

3.3. Kinetic study of dalcochinase mutants

The catalytic efficiencies of the recombinant wild-type and mutant forms of dalcochinase for the hydrolysis of *p*NP-glycoside substrates were determined by substrate-depletion assays (Table 1). These k_{cat}/K_m values of each substrate were then used to calculate the differences in the activation free energy for the formation of glycosyl-enzyme intermediates ($\Delta\Delta G^{\ddagger}$) as a result of each mutation (Fig. 2). Comparison of catalytic efficiencies, thus active site specificities, between two enzymes for a range of substrates is best achieved through the LFER plot, which is a plot of log k_{cat}/K_m of each substrate for one enzyme versus the same parameter for the other enzyme (Supplementary Fig. 5). Such a plot essentially directly compares the free energy of activation for each enzyme/substrate pair, thus constitutes a linear free energy relationship.[36] In such a plot, the correlation coefficient and slope provide measures of the similarities of the two active sites, with values of 1 in each case indicating extremely high similarity or identity. The absolute efficiencies of the two enzymes are not captured in these numbers—but rather in relative k_{cat}/K_m values for a single substrate. The LFER plot between the two wild-type enzymes showed a slope of 1.0 and a correlation coefficient of 0.88, revealing the high similarity of the two active sites (Table 2 and Supplementary Fig. 5).

Among the mutants created and kinetically characterized, the only one with substantially improved kinetic parameters is the Fl96H mutant, which has essentially identical catalytic efficiency to that of the wild-type enzyme for *p*NP-β-D-Glc, but has efficiencies of up to 3-fold higher for *p*NP-β-D-Man and approximately 2-fold higher for most other substrates (Table 1). This result fits well with the location of its corresponding position F205 in the active site of *Z. mays* (maize) β-glucosidase ZmGlu1, near the 2-position of its natural substrate DIMBOA- β-D-glucoside.[17,40] Additionally, this position corresponds to H195 and H193 in *Hordeum vulgare* L. (barley) HvBII and rice Os7BGlu26, respectively, both of which showed preferences for *p*NP-β-D-Man over *p*NP-β-D-Glc, but are N190 and D191 in rice Os3BGlu7 and Os3BGlu8, respectively, which are primarily β-glucosidases.[38] Presumably, improved hydrogen bonding or Van der Waals interactions at the transition state as a result of the F196H substitution bring about this improved behavior. In comparison to the previous study, the substitution of aspartate at the conserved residue N206 in *Pyrococcus furiosus* β-glucosidase did not increase its efficiency toward *p*NP-β-D-Man (49.8 and 3.1 s^{-1} mM^{-1} for the wild-type enzyme and the N206D mutant, respectively), but its preference for mannoside:glucoside increased 18-fold (from 0.7:100 to 13:100 for the wild-type enzyme and the N206D mutant, respectively).[25] In this study, the substitution of histidine at the non-conserved residue F196 in dalcochinase not only increased its efficiency toward *p*NP-β-D-Man (0.06 and 0.17 s^{-1} mM^{-1} for the wild-type enzyme and the F196H mutant, respectively), but also improve its preference for mannoside:glucoside about 3-fold (from 0.5:100 to 1.3:100 for the wild-type enzyme and the F196H mutant, respectively). The difference may lie in the fact that the N206D mutation in *P. furiosus* β-glucosidase resulted in about 300-fold reduction in efficiency for hydrolysis of *p*NP-β-D-Glc but only 16-fold reduction

Table 1
Catalytic efficiencies for hydrolysis of *p*NP-glycosides by the recombinant wild-type and mutant forms of dalcochinase

Enzyme	k_{cat}/K_m (s^{-1} mM^{-1})					
	*p*NP-β-D-Glc	*p*NP-β-D-Fuc	*p*NP-α-L-Ara	*p*NP-β-D-Gal	*p*NP-β-D-Xyl	*p*NP-β-D-Man
Wild-type	13.772 ± 0.003	65.0 ± 0.1	0.844 ± 0.001	0.3898 ± 0.0002	0.260 ± 0.001	0.0628 ± 0.0002
F196H	13.59 ± 0.02	74 ± 5	1.63 ± 0.01	0.6340 ± 0.0002	0.4615 ± 0.0003	0.1731 ± 0.0002
S251V	3.277 ± 0.003	18.7 ± 0.1	0.376 ± 0.001	0.1822 ± 0.0001	0.1214 ± 0.0001	N.D.[a]
M369E	7.52 ± 0.01	51.9 ± 0.1	0.5000 ± 0.0003	0.500 ± 0.002	0.2260 ± 0.0004	0.0558 ± 0.0002
F196H/S251V	9.64 ± 0.01	45.6 ± 0.3	0.4079 ± 0.0003	0.2225 ± 0.0003	0.1483 ± 0.0002	0.0114 ± 0.0001
F196H/M369E	7.56 ± 0.01	42.7 ± 0.4	0.845 ± 0.001	0.282 ± 0.003	0.080 ± 0.001	0.0274 ± 0.0001
S251V/M369E	6.5 ± 0.1	35 ± 1	0.526 ± 0.001	0.2339 ± 0.0003	0.117 ± 0.001	0.01386 ± 0.00002
F196H/S251V/M369E	5.19 ± 0.01	30.4 ± 0.2	0.3178 ± 0.0003	0.1059 ± 0.0004	0.1059 ± 0.0001	0.00786 ± 0.00003

[a] N.D., no absorbance change was detected during overnight incubation.

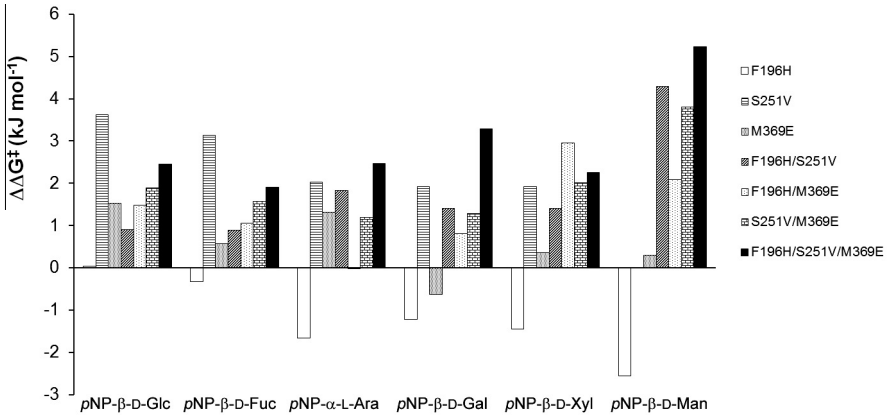

Figure 2. The differences in the activation free energy ($\Delta\Delta G^{\ddagger}$) for the formation of the $ES^{\ddagger}$ complex between the mutant and the recombinant wild-type dalcochinase. Note that the value of $\Delta\Delta G^{\ddagger}$ of the S251V mutant toward pNP-β-D-Man is absent in this plot because the catalytic efficiency could not be determined.

Table 2
Parameters of LFER plots between the log k_{cat}/K_m for the recombinant wild-type and mutant forms of dalcochinase versus the corresponding value for Abg

LFER parameter	Dalcochinase forms							
	wild-type	F196H	S251V	M369E	F196H/S251V	F196H/M369E	S251V/M369E	F196H/S251V/M369E
Slope	1.01	0.87	0.84	0.94	1.15	1.09	1.09	1.10
Correlation coefficient (R^2)	0.88	0.86	0.80	0.85	0.88	0.91	0.89	0.86

in efficiency for hydrolysis of *p*NP-β-D-Man, whereas for the F196H mutation in dalcochinase, the catalytic efficiency for hydrolysis of *p*NP-β-D-Glc was not significantly affected while the efficiency for hydrolysis of *p*NP-β-D-Man increased 3-fold. So, it is possible that the conserved residue N206 in *P. furiosus* β-glucosidase, corresponding to N181 in dalcochinase, plays a dominant role in both binding and catalysis of the glycoside substrate.

Ironically, however, although improving catalytic efficiencies, the F196H mutation does not make the enzyme more Abg-like, but rather worsens the correlation in the LFER—with a slope of 0.87 and a correlation coefficient of 0.86 (Table 2 and Supplementary Fig. 5). With the exception of the M369E mutation, which improves catalytic efficiency for *p*NP-β-D-Gal by 25% (while decreasing efficiencies for all other substrates), all other mutations proved to be deleterious. This is reflected graphically in Fig. 2, which shows changes in activation free energy for each substrate/mutant pair. Therefore, the generally lower catalytic efficiencies of dalcochinase than Abg for various glycoside substrates do not derive only from differences in "first sphere" active site residues located in the glycone binding pocket, but rather draw from differences in more remote residues in both glycone and aglycone binding pockets that contribute to transition state stabilization, possibly coupled with differences in dynamic behavior, geometry, and electrostatic interactions of the rest of the enzyme.

3.4. Interaction between mutations

The double and triple mutants were created to test the interactions among these 3 positions, following the theory proposed previously.[41] The effects of multiple mutations were interpreted based on the differences in the activation energy for the formation of the glycosyl-enzyme intermediates ($\Delta\Delta G^{\ddagger}$, from k_{cat}/K_m values) between the wild-type and mutant enzymes as shown in Fig. 2. In this principle, the effects of the two single mutations ($\Delta\Delta G^{\ddagger}_1$ and $\Delta\Delta G^{\ddagger}_2$, where $\Delta\Delta G^{\ddagger}_1 > \Delta\Delta G^{\ddagger}_2$) were compared with the effect of the double mutation ($\Delta\Delta G^{\ddagger}_{1+2}$) and the sum of the effects of the two single mutations ($\Delta\Delta G^{\ddagger}_1 + \Delta\Delta G^{\ddagger}_2$). Interactions of two mutations can be classified into one of five categories, which are addition, partial addition, antagonism, synergism, and no effect.[41,42]

The analysis of the interactions between mutations performed in this study is shown in Table 3 (and detailed analysis shown in Supplementary Table 3). For most pairs of mutations, antagonistic

Table 3
Analysis of the interactions between mutations performed in this study

Substrate	F196H/ S251V	F196H/ M396E	S251V/ M369E	F196H/ S251V/ M369E
*p*NP-β-D-Glc	Antagonism	Antagonism	Antagonism	Antagonism
*p*NP-β-D-Fuc	Antagonism	Synergism	Antagonism	Antagonism
*p*NP-α-L-Ara	Antagonism	Antagonism	Antagonism	Synergism
*p*NP-β-D-Gal	Antagonism	Synergism	Antagonism	Synergism
*p*NP-β-D-Xyl	Antagonism	Synergism	Partial addition	Antagonism
*p*NP-β-D-Man	Antagonism	Synergism	Antagonism	Antagonism

interactions, in which the effects of the double mutations were less than the effects of the more damaging single mutation, were observed, suggesting that these mutations represented opposing structural effects on the same catalytic step such that the effect of one mutation would partially rescue the damaging effect of the other mutation. On the other hand, synergistic interactions, in which the effects of the double mutations exceeded the sum of the effects of the two single mutations, were observed in six cases. Synergism can be caused by three conditions; (1) anti-cooperative interaction of residues that introduce strain into the transition state of the same rate-limiting step, (2) extensive unfolding of enzyme as a result of the double mutations, or (3) noninteracting residues that slow down the same non rate-limiting step such that it becomes a rate-limiting step in the double mutant.[41,42] The first condition was unlikely as F196 and M369 were placed 12.2 Å apart (measured from F196-CZ and M369-Cε) in the dalcochinase model, whereas interacting residues that contribute to a change in $\Delta\Delta G^{\ddagger}$ should be located within 4 Å to be in Van der Waals contact.[43] The second condition was also unlikely as the kinetic parameters for these mutants are roughly comparable to those of the wild-type enzyme. So, the third condition seemed the most likely explanation for the synergistic interaction between these positions. Lastly, a partially additive effect, in which the effect of the double mutations was greater than the effect of the more damaging single mutation alone but still lower than the sum of the effects of the two single mutations, was observed in the hydrolysis of pNP-β-D-Xyl by the S251V/M369E mutant. Partially additive interactions could be due to (1) partially cooperative interactions between residues in the same step, or (2) independent residues acting in the consecutive non rate-limiting steps.[41,42] Since these residues were placed 14.16 Å apart (measured from S251-OG and M369-Cε) in the dalcochinase model, only the second explanation is possible.

4. Conclusion

Mutations of the residues in the glycone binding pocket of dalcochinase to those of Abg showed that the F196H mutation could improve the activity of the enzyme on some substrates, especially the mannoside. This is consistent with the fact that two other GH1 glycosidases (barley HvBII and rice Os7Bglu26), which prefer β-mannosides over β-glucosides as substrates, both naturally have histidine at this position. Presumably, the histidine residue is able to form an improved hydrogen bond with manno-configured substrates at the transition state for the glycosylation step. Since hydrogen bond interactions between the hydroxyl group at the C-2 position and the residues in the active site pocket of the enzyme contribute directly to transition state stabilization, our result has implications for the molecular mechanism for determining glycone specificity in other GH1 β-glucosidases. However, other mutations made the enzyme less Abg-like in its substrate specificity. So, the behavior of the enzyme is not only determined by the presence of unique amino acid residues, but also their context in the overall active site architecture, including interactions with remote residues, geometry, and electrostatic field of the rest of the enzyme.

Acknowledgments

The authors especially thank Watchara Kasinrerk for providing the mouse monoclonal antibody against natural dalcochinase. The project was financially supported by Grants from the Thailand Research Fund and the Commission on Higher Education (RMU5480004); the Commission on Higher Education; Kasetsart University Research and Development Institute (V-T(D)22.50); the Higher Education Research Promotion and National Research University Project of Thailand; the Faculty of Science (ScRF-S2-18/2551) and the Graduate School, Kasetsart University; and the Natural Sciences and Engineering Research Council of Canada. K.R. and K.C. are recipients of the Ph.D. scholarships from the Commission on Higher Education, Thailand.

Supplementary data

Supplementary data associated with this article can be found, in the online version, at http://dx.doi.org/10.1016/j.carres.2012.10.018.

References

1. Henrissat, B.; Bairoch, A. *Biochem. J.* **1996**, *316*, 695–696.
2. Ketudat Cairns, J. R.; Esen, A. *Cell. Mol. Life Sci.* **2010**, *67*, 3389–3405.
3. www.cazy.org/Glycoside-Hydrolases.html.
4. Esen, A. β-Glucosidase: Overview. In *β-Glucosidase Biochemistry and Molecular Biology*; Esen, A., Ed.; American Chemical Society: Washington, DC, 1992; pp 1–14.
5. McCarter, J. D.; Withers, S. G. *Curr. Opin. Struct. Biol.* **1994**, *4*, 885–892.
6. Ketudat-Cairns, J. R.; Champattanachai, V.; Srisomsap, C.; Wittman-Liebold, B.; Thiede, B.; Svasti, J. *J. Biochem.* **2000**, *128*, 999–1008.
7. Svasti, J.; Srisomsap, C.; Techasakul, S.; Surarit, R. *Phytochemistry* **1999**, *50*, 739–743.
8. Srisomsap, C.; Svasti, J.; Surarit, R.; Champattanachai, V.; Sawangareetrakul, P.; Boonpuan, K.; Subhasitanont, P.; Chokchaichamnankit, D. *J. Biochem.* **1996**, *119*, 585–590.
9. Wakarchuk, W. W.; Kilburn, D. G.; Miller, R. C., Jr; Warren, R. A. J. *Mol. Gen. Genet.* **1986**, *205*, 146–152.
10. Day, A. G.; Withers, S. G. *Biochem. Cell Biol.* **1986**, *64*, 914–922.
11. Withers, S. G.; Rupitz, K.; Trimbur, D.; Warren, R. A. J. *Biochemistry* **1992**, *31*, 9979–9985.
12. Wang, Q.; Trimbur, D.; Graham, R.; Warren, R. A. J.; Withers, S. G. *Biochemistry* **1995**, *34*, 14554–14562.
13. Kempton, J. B.; Withers, S. G. *Biochemistry* **1992**, *31*, 9961–9969.
14. Rivera-Sagredo, A.; Canada, F. J.; Nieto, O.; Jimenez-Barbero, J.; Martin-Lomas, M. *Eur. J. Biochem.* **1992**, *209*, 415–422.
15. Namchuk, M. N.; Withers, S. G. *Biochemistry* **1995**, *34*, 16194–16202.
16. Barrett, T.; Suresh, C. G.; Tolley, S. P.; Dodson, E. J.; Hughes, M. A. *Structure* **1995**, *3*, 951–960.
17. Czjzek, M.; Cicek, M.; Zamboni, V.; Burmeister, W. P.; Bevan, D. R.; Henrissat, B.; Esen, A. *Biochem. J.* **2001**, *354*, 37–46.
18. Corbett, K.; Fordham-Skelton, A. P.; Gatehouse, J. A.; Davis, B. G. *FEBS Lett.* **2001**, *509*, 355–360.
19. Marana, S. R.; Jacobs-Lorena, M.; Terra, W. R.; Ferreira, C. *Biochim. Biophys. Acta* **2001**, *1545*, 41–52.
20. Verdoucq, L.; Morinière, J.; Bevan, D. R.; Esen, A.; Vasella, A.; Henrissat, B.; Czjzek, M. *J. Biol. Chem.* **2004**, *279*, 31796–31803.
21. Isorna, P.; Polaina, J.; Latorre-García, L.; Cañada, F. J.; González, B.; Sanz-Aparicio, J. *J. Mol. Biol.* **2007**, *371*, 1204–1218.
22. Nijikken, Y.; Tsukada, T.; Igarashi, K.; Samejima, M.; Wakagi, T.; Shoun, H.; Fushinobu, S. *FEBS Lett.* **2007**, *581*, 1514–1520.
23. Chuenchor, W.; Pengthaisong, S.; Robinson, R. C.; Yuvaniyama, J.; Oonanant, W.; Bevan, D. R.; Esen, A.; Chen, C.-J.; Opassiri, R.; Svasti, J.; Cairns, J. R. K. *J. Mol. Biol.* **2008**, *377*, 1200–1215.
24. Tribolo, S.; Berrin, J.-G.; Kroon, P. A.; Czjzek, M.; Juge, N. *J. Mol. Biol.* **2007**, *370*, 964–975.
25. Kaper, T.; Van Heusden, H. H.; Van Loo, B.; Vasella, A.; Van der Oost, J.; De Vos, W. M. *Biochemistry* **2002**, *41*, 4147–4155.
26. Toonkool, P.; Metheenukul, P.; Sujiwattanarat, P.; Paiboon, P.; Tongtubtim, N.; Ketudat-Cairns, M.; Ketudat-Cairns, J.; Svasti, J. *Protein Expr. Purif.* **2006**, *48*, 195–204.

27. Thompson, J. D.; Higgins, D. G.; Gibson, T. J. *Nucleic Acids Res.* **1994**, *22*, 4673–4680.
28. Eswar, N.; Webb, B.; Marti-Renom, M. A.; Madhusudhan, M. S.; Eramian, D.; Shen, M. Y.; Pieper, U.; Sali, A. *Curr. Protoc. Protein Sci.* **2007**, *50*, 2.9.1–2.9.31.
29. Luthy, R.; Bowie, J. U.; Eisenberg, D. *Nature* **1992**, *356*, 83–85.
30. Laskowski, R. A.; MacArthur, M. W.; Moss, D. S.; Thornton, J. M. *J. Appl. Cryst.* **1993**, *26*, 283–291.
31. Wiederstein, M.; Sippl, M. J. *Nucleic Acids Res.* **2007**, *35*, 407–410.
32. Kongsaeree, P. T.; Ratananikom, K.; Choengpanya, K.; Tongtubtim, N.; Sujiwattanarat, P.; Porncharoennop, C.; Onpium, A.; Svasti, J. *J. Mol. Catal. B: Enzyme* **2010**, *67*, 257–265.
33. Charoenrat, T.; Ketudat-Cairns, M.; Jahic, M.; Enfors, S.-O.; Veide, A. *J. Biotechnol.* **2006**, *122*, 86–98.
34. Laemmli, U. K. *Nature* **1970**, *227*, 680–685.
35. Wicki, J.; Schloegl, J.; Tarling, C. A.; Withers, S. G. *Biochemistry* **2007**, *46*, 6996–7005.
36. Withers, S. G.; Rupitz, K. *Biochemistry* **1990**, *29*, 6405–6409.
37. Burmeister, W. P.; Cottaz, S.; Rollin, P.; Vasella, A.; Henrissat, B. *J. Biol. Chem.* **2000**, *275*, 39385–39393.
38. Kuntothom, T.; Luang, S.; Harvey, A. J.; Fincher, G. B.; Opassiri, R.; Hrmova, M.; Ketudat Cairns, J. R. *Arch. Biochem. Biophys.* **2009**, *491*, 85–95.
39. Cereghino, J. L.; Cregg, J. M. *FEM Microbiol. Rev*. **2000**, *24*, 45–66.
40. Hill, A. D.; Reilly, P. J. *Biopolymers* **2008**, *89*, 1021–1031.
41. Mildvan, A. S.; Weber, D. J.; Kuliopulos, A. *Arch. Biochem. Biophys.* **1992**, *294*, 327–340.
42. Mildvan, A. S. *Biochemistry* **2004**, *43*, 14517–14520.
43. Wells, J. A. *Biochemistry* **1990**, *29*, 8509–8517.
44. Hancock, S. M.; Corbett, K.; Fordham-Skelton, A. P.; Gatehouse, J. A.; Davis, B. G. *ChemBioChem* **2005**, *6*, 866–875.